

DO BLACK HOLE CANDIDATES HAVE MAGNETIC MOMENTS INSTEAD OF EVENT HORIZONS?

STANLEY L. ROBERTSON¹ AND DARRYL J. LEITER²

Draft version January 16, 2019

ABSTRACT

In previous work we found that many of the spectral properties of low mass x-ray binaries (LMXB), including galactic black hole candidates (GBHC) were consistent with the existence of intrinsically magnetized central objects. We review and extend these findings and show that the existence of intrinsically magnetic BHC is consistent with a new class of solutions of the Einstein field equations of General Relativity. These solutions are based on a strict adherence to the Strong Principle of Equivalence (SPOE) requirement that the world lines of physical matter must remain timelike in all regions of spacetime. The new solutions emerge when the structure and radiation transfer properties of the energy momentum tensor on the right hand side of the Einstein field equations are appropriately chosen to dynamically enforce the SPOE requirement of timelike world line completeness. In this context, we find that the Einstein field equations allow the existence of highly red shifted, Magnetospheric, Eternally Collapsing Objects (MECO). MECO can possess intrinsic magnetic moments since they do not have trapped surfaces that lead to event horizons and curvature singularities. Since MECO lifetimes are orders of magnitude greater than a Hubble time, they provide an elegant and unified framework for understanding a broad range of observations of GBHC and active galactic nuclei. We examine their properties and discuss characteristics that might lead to their confirmation.

Subject headings: Accretion, Black Holes, Active Galaxies, Stars: neutron, Stars: novae, X-rays: stars

1. INTRODUCTION

In earlier work (Robertson & Leiter 2002) we presented evidence for the existence of intrinsic magnetic moments of $\sim 10^{29}$ G cm³ in galactic black hole candidates (GBHC). These findings are recapitulated and extended in Table 1 and Appendix D, which summarizes the equations and the analysis of observations. Combined with rotation rates in the range 10 - 50 Hz, these magnetic moments provide a robust unified mechanism for the spectral state switches observed in GBHC and neutron stars (NS), a common origin of quiescent power-law emissions as spin-down luminosity, and a unified driving mechanism for the ubiquitous low-state jets and synchrotron emissions of both. Magnetosphere topology also serves to stabilize the inner accretion disk (Arons et al. 1984). The great strength of the magnetospheric model that we describe is that it allows a unified description of all of the various spectral and luminosity states of x-ray novae, whether NS or GBHC. Similarities of NS and GBHC properties, particularly in low and quiescent states, have been previously noted, (e.g. van der Klis 1994, Tanaka & Shibazaki 1996) as well as the lack of compelling evidence for event horizons (Abramowicz, Kluzniak & Lasota 2002). The central question at this point is, what is the nature of the compact objects that we call GBHC.

There is a plethora of piece meal models of these various phenomena. For example, comptonizing coronae near event horizons, bulk flow comptonization and magnetic flares on accretion disks have all been invoked to explain the hard spectral tail of low state GBHC. But the observed ingress/egress times for dipping sources imply large radiating regions (Church 2001) that are inconsistent with

the compact corona models and can be consistent with bulk comptonization models only for large scale outflows. Similarly, radiatively inefficient advective flows at high accretion rates have been proposed to explain the quiescent power-law emissions of GBHC, (Narayan et al. 1997, Garcia et al. 2001). while ignoring the fact that the similar emissions of accreting millisecond pulsars are adequately explained by magnetospheric spin-down. Stated more bluntly, Cir X-1, a burster with a magnetic moment similar to those found for GBHC (Table 1 and Iaria et al. 2001), exhibits essentially all of the x-ray spectral and timing characteristics that have been proposed at various times as distinguishing features of black holes. A unified model of GBHC and NS that can be used to clarify subtle differences is clearly needed.

Others have reported evidence for strong magnetic fields in GBHC. A field in excess of 10^8 G has been found at the base of the jets of GRS 1915+105 (Gliozzi, Bodo & Ghisellini 1999, Vadawale, Rao & Chakrabarti 2001). A recent study of optical polarization of Cygnus X-1 in its low state (Gnedin et al. 2003) has found a slow GBHC spin and a magnetic field of $\sim 10^8$ gauss at the location of its optical emission. Given the r^{-3} dependence of field strength on magnetic moment, the implied magnetic moments are in good agreement with those we have found. A recent correlation (Mauche et al. 2002, Warner & Woudt 2003) of quasi-periodic oscillation (QPO) frequencies extending over six orders of magnitude in frequency, from dwarf novae to neutron stars shows points for GBHC squarely in the middle of the line. If the higher of the correlated frequencies is generated where the inner radius of an accretion disk interacts with a magnetosphere (Goodson, Bohm

¹Dept. of Physics, Southwestern Oklahoma State University, Weatherford, OK 73096

²FSTC, Charlottesville, VA 22901

& Winglee 1999, Titarchuk & Wood 2002), this would be additional evidence of intrinsic magnetic moments for GBHC. A relativistic frame-dragging explanation is surely not applicable.

While accommodating intrinsic magnetic moments in models of GBHC would require revisions in the current theoretical picture of these compact objects, such an approach would also greatly simplify the problem of understanding the spectral, timing and jet ejection mechanisms of compact objects. If GBHC have intrinsic magnetic moments that are not generated by external currents in an accretion disk, then they would not possess event horizons. As noted by Abramowicz, Kluzniak & Lasota (2002), it is unlikely that we will ever find direct observational proof of an event horizon, however, we may be able to observationally determine whether or not GBHC have intrinsic magnetic moments. If GBHC are not black holes, they would almost certainly be magnetized and likely to at least a degree similar to their compact NS cousins.

Although there are widely studied models for generating magnetic fields in accretion disks, most can produce equipartition fields at best (Livio & Pringle 1999), perhaps at the expense of being too luminous (Bisnovatyi-Kogan & Lovelace 2000) in quiescence. While tangled magnetic fields in accretion disks are very likely responsible for their large viscosity, (e.g. Hawley, Balbus & Winters 1999) the highly variable mass accretion rates in LMXB make it unlikely that disk dynamos could produce the stability of fields needed to account for either spectral state switches or quiescent spin-down luminosities. Both also require magnetic fields co-rotating with the central object. Further, if disk dynamos produced the much larger apparent magnetic moments of GBHC, they should produce them also for the NS systems and cause profound qualitative spectral and timing differences via interactions with the intrinsic NS magnetic moments. Such qualitative differences as have been observed, e.g., the hard spectral tail of the high/soft state, lack of surface bursts for GBHC and stronger GBHC jets, are easily explained by differences in masses and magnetic field strengths. Not only are there are no observed differences that require explanation in terms of event horizons (Abramowicz, Kluzniak & Lasota 2002), there appear to be none that would be consistent with having two different magnetic structures for NS and GBHC.

It has been suggested that stable magnetic fields could be produced by electrically charged, rotating black holes (Punsley 1998, Gnedin et al. 2003), however the charge necessary to endow Cygnus X-1 with a 10^8 G magnetic field, well out in the accretion disk, was found to be 5×10^{28} esu (Gnedin et al. 2003). Due to the large charge/mass ratios of accreting protons or electrons, this quantity of black hole charge would produce electric forces at least $\sim 10^6$ larger than the gravitational attraction of $10M_{\odot}$,

thus causing charges of one sign to be swallowed and the other to be blown away. At accretion rates needed to account for the x-ray luminosity of Cygnus X-1, the original charge would be neutralized in a fraction of one second. Thus it appears that current black hole models are unable to offer unified explanations of such obviously magnetic phenomena as jets, spectral state switches and quiescent synchrotron emissions and if they could, it seems unusually generous for nature to have provided different mechanisms for NS and GBHC to produce such strikingly similar phenomena.

2. THE STRONG PRINCIPLE OF EQUIVALENCE

Astrophysicists nowadays generally accept the inevitability of the curvature singularities of black holes, however, if the GBHC are intrinsically magnetized, this will be nature's way of telling us that such singularities are not really permitted to exist. If so, we are left with the task of finding a fundamental reason for their prohibition. In General Relativity (GR) the strong principle of equivalence (SPOE) requires that Special Relativity (SR) must hold locally for freely falling time-like observers in all of spacetime. This SPOE requirement is a tensor relationship that implies that (i) the spacetime manifold for observers located in field-free regions, distant from gravitating masses, must approach the flat spacetime of SR and (ii) the spacetime world lines of massive matter must always be timelike.³ Such spacetime manifolds are known as 'bundle complete' (Wheeler & Ciufolini 1995).

As a guiding principle, we look for solutions of the Einstein equations that satisfy the SPOE requirement that the world lines of physical matter under the influence of both gravitational and non-gravitational forces must not be allowed to become null or spacelike in any region of spacetime. Since the energy-momentum tensor serves as both a source of curvature in the Einstein equations and a generator of the equations of motion of matter, any constraints on the latter will affect the former. Hence to assure 'timelike world line completeness', the right hand side of the GR field equation

$$G^{\mu\nu} = (8\pi G/c^4)T^{\mu\nu} \quad (1)$$

must contain non-gravitational elements capable of stopping the collapse of physical matter before the formation of a 'trapped surface', thus dynamically avoiding the Hawking and Penrose theorem which states that once a trapped surface is formed, an event horizon and curvature singularities are unavoidable.

In this context, we have found that it is possible to virtually stop and maintain a collapsing compact physical plasma object outside of its Schwarzschild radius with photon pressure generated by synchrotron radiation from an equipartition magnetic field, though the object must then radiate at the local Eddington limit. There is strong recent

³Models of gravitational collapse that lead to the development of event horizons and central curvature singularities inevitably abandon the SPOE requirement for timelike world line completeness. The vanishing of the metric coefficient g_{tt} at the Schwarzschild radius is sufficient to cause free-fall geodesics of test particles in non-singular Finkelstein or Kerr-Schild coordinates, for constant central mass, to become null at the event horizon, though the crossing can at least be accomplished in a finite coordinate time, as well as proper time, for Kerr-Schild. See Appendix A. It has been shown (Leiter & Robertson 2003) that null geodesics occur at surfaces of infinite redshift. In Kruskal-Szekeres coordinates, in which g_{tt} does not vanish, there is no surface of infinite redshift at the Schwarzschild radius and timelike test particle geodesics can traverse it *in either direction*, so long as the initial conditions are chosen in a manner that permits the 'time' coordinate to change in a positive sense. However, a central singularity still exists in these coordinates and they cannot apply to a gravitational collapse process (Weinberg 1972, Rindler 1977) nor can they describe the distant asymptotically flat spacetime. They do, however, have a surface of infinite redshift as $r \rightarrow \infty$, at which outgoing geodesics become null. Thus they appear to have no applicability to astrophysics.

evidence for the presence of such extreme magnetic fields in gravitational collapse. Equipartition magnetic fields have been implicated as the driver of GRB 021206 (Coburn & Boggs 2003) and strong residual fields much in excess of those expected from mere flux compression during stellar collapse have been found in magnetars (Ibrahim, Swank & Parke 2003). Kluzniak and Ruderman (1998) have described the generation of $\sim 10^{17}$ G magnetic fields via differential rotation in neutron stars. It is likely that larger fields might be generated for the more massive GBHC. An equipartition field would have $B^2/8\pi \sim \rho c^2/3$, where B is magnetic field strength and ρ the mass density. Generating $B \sim 10^{18}$ G, for nuclear densities, should be possible via differential rotation and relativistic field compression as surface redshift increases from the vicinity of $z \gtrsim 0.1$ during the final adiabatic decay of core neutrino emissions. Other possibilities for producing extreme magnetic fields would include ferromagnetic phase transitions during the collapse (Haensel & Bonazzola 1996, J. Noble private communication) or the formation of quark condensates. Fields of this order have been modeled for quark condensates (Tatsumi 2000), who notes that quark liquids can undergo a ferromagnetic phase transition at densities as low as nuclear saturation. An equipartition magnetic field seems to be a necessary part of a mechanism to ensure the SPOE requirement for timelike worldline completeness.⁴

At the temperatures and compactness of stellar collapse, a pair plasma is produced. Pelletier & Marcowith (1998) have shown that the energy density of magnetic perturbations in equipartition pair plasmas is preferentially converted to photon pressure, rather than causing particle acceleration. The radiative power of an equipartition pair plasma is proportional to B^4 , (pair density $\propto B^2$ and synchrotron energy production $\propto B^2$.) Lacking the equipartition pair plasma, magnetic stress, $B^2/8\pi$, and gravitational stress, $GM\rho/R$, on mass density ρ , would both increase as R^{-4} during gravitational collapse. Magnetic fields below equipartition levels would be incapable of stopping the collapse. However, since photon pressure generated by the pairs at equipartition increases more rapidly than gravitational stresses, it is possible to stabilize the rate of collapse at an Eddington limit rate. With this extremely efficient photon production mechanism, the radiation temperature is buffered near the pair production threshold. In effect, the rate of collapse is buffered by a phase transition. For equipartition conditions, the field also exceeds that required to confine the pair plasma. A stable rate of collapse is maintained by increased (decreased) photon pressure ($\propto B^4$) if the field is increased (decreased) by compression or expansion. Since the photon luminosity is not confined to the core it will not be trapped, as occurs with neutrinos, however, the radiation should be thermalized as it diffuses through an optically thick environment. *To reduce the field to the distantly observed levels implied by our previous GBHC studies would require the existence of a red shift of $z \sim 10^8$. Thus we are motivated by the SPOE to look for solutions of the GR field equations that are consistent with Eddington limited, highly redshifted, gravitational collapse.* The residual,

distantly observed magnetic moment and extremely faint, redshifted radiations would be the only things that would distinguish such an object from a black hole (Abramowicz, Kluzniak & Lasota 2002).

In Section 3 we show that strict enforcement of the SPOE requirement for timelike world line completeness leads to a ‘no trapped surface’ condition. In Section 4 we show that the gravitational collapse of a magnetospheric, eternally collapsing object (MECO) that radiates at its local Eddington limit would continue for a duration exceeding a Hubble time. In Sections 5 - 10, we examine other physical characteristics of MECO.

3. A STRICT INTERPRETATION OF SPOE REQUIRES MECO

The simplest form of the energy-momentum tensor, which can satisfy the SPOE requirement of time like world line completeness, is one which describes a collapsing, radiating plasma containing equipartition magnetic fields which emit outgoing radiation. Between the extremes of pure magnetic energy (Thorne 1965) and weakly magnetic, radiation dominated polytropic gases or pressureless dust (Baumgarte & Shapiro 2003) there should be cases where the rate of collapse can be stable. To first order, in an Eddington limited radiation dominated context, these can be described by the energy momentum tensor:

$$T_{\mu}^{\nu} = (\rho + P/c^2)u_{\mu}u^{\nu} - P\delta_{\mu}^{\nu} + E_{\mu}^{\nu} \quad (2)$$

where $E_{\mu}^{\nu} = Qk_{\mu}k^{\nu}$, $k_{\mu}k^{\mu} = 0$ describes outgoing radiation in a geometric optics approximation, ρ is energy density of matter and P the pressure. Energy momentum tensors corresponding to metrics describing ingoing radiation, which are used in many black hole model calculations, (e.g. Baumgarte & Shapiro 2003) cannot be used here because they are incompatible with the $Q > 0$ boundary conditions associated with collapsing, outwardly radiating objects.

We choose a comoving interior metric given by

$$ds^2 = A(r, t)^2 c^2 dt^2 - B(r, t)^2 dr^2 - R(r, t)^2 (d\theta^2 + \sin^2\theta d\phi^2) \quad (3)$$

and an exterior Vaidya metric with outgoing radiation

$$ds^2 = (1 - 2GM/c^2 R) c^2 du^2 + 2cdudR - R^2 (d\theta^2 + \sin^2\theta d\phi^2) \quad (4)$$

where R is the areal radius and $u = t - R/c$ is the retarded observer time. Following Lindquist, Schwarz & Misner (1965), we define

$$\Gamma = \frac{dR}{dl} \quad (5)$$

$$U = \frac{dR}{d\tau} \quad (6)$$

$$M(r, t) = 4\pi \int_0^r \rho R^2 \frac{dR}{dr} dr \quad (7)$$

$$\Gamma^2 = \left(\frac{dR}{dl}\right)^2 = 1 - \frac{2GM(r, t)}{c^2 R} + \frac{U}{c} \quad (8)$$

where dl is a proper length element in a zero angular momentum comoving frame, $d\tau$ an increment of proper time,

⁴Work by Baumgarte & Shapiro (2003) and Thorne (1965) have explored differing cases of magnetic field strength. The former considers a pressureless dust with matter gravitation dominating the magnetic field and finds a collapse to a black hole state (that nevertheless violates timelike world line completeness.) As recounted by Thorne (1994) dipole-like magnetic fields without rest mass do not collapse to form trapped surfaces. These results should heighten the interest in detailed numerical calculations for a radiating equipartition case.

U is the proper time rate of change of the radius associated with the invariant circumference of the collapsing mass, and $M(r, t)$ is the mass enclosed within this radius. The last two of the relations above have been obtained from the G_0^0 component of the field equation (Lindquist, Schwarz & Misner 1965). At the boundary of the collapsing, radiating surface, s , we find that the proper time will be positive definite, as required for timelike world line completeness if

$$d\tau_s = \frac{du}{1+z_s} = du \left(\left(1 - \frac{2GM(r, t)_s}{c^2 R_s} + \frac{U_s}{c}\right)^{1/2} + \frac{U_s}{c} \right) > 0 \quad (9)$$

where z_s is the distantly observed redshift of the collapsing surface. From Equation (9) we see that in order to avoid a violation of the requirement of timelike world line completeness for $U_s < 0$, it is necessary to dynamically enforce the ‘no trapped surface condition’⁵:

$$\frac{2GM_s}{c^2 R_s} < 1 \quad (10)$$

Since there is nothing in the Einstein tensor $G^{\mu\nu}$ that enforces this condition, we must rely on non-gravitational forces in $T^{\mu\nu}$ to enforce the SPOE condition of time like world line completeness. For the MECO model, we use radiation pressure where

$$Q = \frac{-(dM/du)/4\pi R^2}{(\Gamma_s + U_s/c)^2} \quad (11)$$

At the comoving MECO surface the luminosity is

$$L = 4\pi R^2 Q > 0. \quad (12)$$

and the distantly observed luminosity is

$$L_\infty = -c^2 \frac{dM_s}{du} = -c^2 \frac{dM_s}{d\tau} (1+z_s) \quad (13)$$

4. EDDINGTON LIMITED MECO

Among the various equations associated with the collapse process there are three proper time differential equations applicable to a compact collapsing and radiating physical surface. When evaluated on the physical surface (Hernandez Jr. & Misner, 1966, Lindquist, Schwartz & Misner 1965, Misner 1965, Lindquist, 1966) these equations are:

$$\frac{dU_s}{d\tau} = \left(\frac{\Gamma}{\rho + P/c^2} \right)_s \left(-\frac{\partial P}{\partial R} \right)_s - \left(\frac{G(M + 4\pi R^3(P + Q)/c^2)}{R^2} \right)_s \quad (14)$$

$$\frac{dM_s}{d\tau} = -(4\pi R^2 P c \frac{U}{c})_s - (L(\frac{U}{c} + \Gamma))_s \quad (15)$$

$$\frac{d\Gamma_s}{d\tau} = \frac{G}{c^4} \left(\frac{L}{R} \right)_s + \frac{U_s}{c^2} \left(\frac{\Gamma}{\rho + P/c^2} \right)_s \left(-\frac{\partial P}{\partial R} \right)_s \quad (16)$$

⁵It might be argued that there might not be a surface that physically divides matter from radiation inside a collapsing massive continuum, however, it has been shown (Mitra 2000, 2002, Leiter & Robertson 2003) that Equations (5 - 8) and the G_0^0 field equation in a zero angular momentum comoving frame produces the ‘no trapped surface condition’ for any interior $R(r, t)$, provided that $B(r, t)$ does not become singular at a location where $A(r, t)$ vanishes. However this requirement will be satisfied as long as timelike world line completeness is maintained by photon pressure generated by the equipartition magnetic field everywhere in the comoving frame. We can consider any interior location and the radiation flux there without requiring a joined Vaidya metric. But there will ultimately be an outer radiating boundary and the required match to the non-singular outgoing exterior Vaidya metric guarantees that there will be no metric singularity there.

In Eddington limited steady collapse, the conditions $dU_s/d\tau = 0$ and $U_s \approx 0$ hold after some time, τ_{edd} , that has elapsed in reaching the Eddington limited state. Then

$$\frac{dU_s}{d\tau} = \frac{\Gamma_s}{(\rho + P/c^2)_s} \left(-\frac{\partial P}{\partial R} \right)_s - \frac{GM_s}{R_s^2} = 0 \quad (17)$$

Where

$$M_s = (M + 4\pi R^3(P + Q)/c^2)_s \quad (18)$$

includes the magnetic field energy in the pressure term and radiant energy in Q .

Equation (17) when integrated over a closed surface can be solved for the net outward flow of Eddington limited luminosity through the surface. Taking the escape cone factor of $27(GM_s/c^2 R_s)^2/(1+z_s)^2$ into account, (See Appendix A) the outflowing (but not all escaping) surface luminosity, L , would be

$$L_{edd}(outflow)_s = \frac{4\pi GM_s c R^2 (1+z_{edd})^3}{27\kappa R_g^2} \quad (19)$$

where $R_g = GM_s/c^2$ and $\kappa \approx 0.4 \text{ cm}^2/g$ is the plasma opacity. (For simplicity, we have assumed here that the luminosity actually escapes from the MECO surface rather than after conveyance through a MECO atmosphere and photosphere. The end result is the same for distant observers.) However the luminosity L_s which appears in equations (15 - 16) is actually the net luminosity, which escapes through the photon sphere, and is given by $L_s = L_{edd}(escape)_s = L_{edd}(outflow) - L_{edd}(fallback) = L_{Edd,s} - L_{Edd,s}(1 - 27R_g^2/(R(1+z_{edd}))^2)$ Thus in equations 15 and 16, the L_s appearing there is given by

$$L_s = L_{edd}(escape)_s = \frac{4\pi GM(\tau)_s c (1+z_{edd})}{\kappa} \quad (20)$$

In this context from (15) we have that

$$c^2 \frac{dM_s}{d\tau} = -\frac{L_{edd}(escape)_s}{(1+z_s)^2} = -\frac{4\pi GM(\tau)_s c}{\kappa} \quad (21)$$

which can be integrated to give

$$M_s(\tau) = M_s(\tau_{edd}) \exp((-4\pi G/\kappa c)(\tau - \tau_{edd})) \quad (22)$$

This yield a distantly observed MECO lifetime of $(1+z_s)\kappa c/4\pi G \sim 5 \times 10^{16} \text{ yr}$ for $z_s \sim 10^8$. Finally, equation (16) becomes

$$\frac{d\Gamma_s}{d\tau} = \frac{G}{c^4} \frac{L_{edd,s}}{R_s(\tau_{edd})} \quad (23)$$

which, in view of (13) has the solution

$$\Gamma_s(\tau) = \frac{1}{1+z_s(\tau)} = \left(1 - \frac{2GM_s(\tau_{edd})}{c^2 R_s(\tau)_{edd}}\right)^{1/2} > 0 \quad (24)$$

which is consistent with (8) and (10).

5. MECO CHARACTERISTICS

If one naively attributes the Eddington limit luminosity to purely thermal processes, one quickly finds that the required MECO surface temperatures would be so high that photon energies would be well beyond the pair production threshold and the compactness would assure that photon-photon collisions would produce numerous electron-positron pairs. Thus the MECO surface region must be dominated by a pair plasma, and at a temperature buffered near the $\sim 6 \times 10^9 K$ threshold for photon-photon collisions to produce pairs (Pelletier & Marcowith 1998). As we shall see, an electron-positron pair atmosphere of a MECO is an extremely significant structure that conveys radiation from the MECO surface to a zone with a much lower red shift and larger escape cone from which it escapes. In order to describe this process computationally within a numerical grid, a radial grid interval no larger than $\sim 10^{-8} R_g$ would be needed, where $R_g = GM/c^2$ is the gravitational radius. Although there have been many numerical studies of the behavior of collapsing compact objects in GR, to our knowledge none have indicated that they have sufficient numerical resolution to examine the extreme red shift regime associated with MECO nor have they considered the emergent properties of equipartition magnetic fields and pair plasmas at high red shift.

The strength of the poloidal component of the intrinsic magnetic fields B_{env} observed in the distant environment around the MECO are reduced by a factor of $(1+z_s)$ from their values near R_s . The fields needed to produce jets in AGN are observed to be of the order $10^3 - 10^4$ gauss as judged distantly. On the other hand, a distantly observed equipartition field would be $\sim 10^{18}/(m(1+z_{edd}))$ gauss, where $m = M/M_\odot$. This suggests that for an $m \sim 10^8$ AGN, the combined effect of mass scaling and red shift would need to reduce the surface field from 10^{18} gauss to 10^{3-4} gauss. This would require the MECO to have a red shift of $z \sim 10^7 - 10^8$. In this and previous work, (Robertson & Leiter 2002) we have found typical magnetic fields of a few times 10^{10} gauss for GBHC. These would require similar values of $z_{edd} \sim 10^8$, as well as $m \sim 10$. Therefore for both GBHC and AGN we find that we need ⁶

$$1 + z_{edd} = \frac{B_{equip}}{B_{env}} \sim 10^8. \quad (25)$$

6. THE QUIESCENT MECO

The quiescent luminosity of a MECO originates deep within its photon sphere. When distantly observed it is diminished by both gravitational red shift and a narrow exit cone. The gravitational red shift reduces the surface luminosity by $1/(1+z)^2$ while the exit cone further reduces the luminosity by the factor $27R_g^2/(R(1+z))^2 \sim 27/(4(1+z)^2)$

⁶An additional point of support for very large values of z concerns neutrino transport in stellar core collapse. If a diffusion limited neutrino luminosity of $\sim 10^{52}$ erg/s (Shapiro & Teukolsky 1983) were capable of very briefly sustaining a neutrino Eddington limit rate of collapse, then the subsequent reduction of neutrino luminosity as neutrino emissions are depleted in the core would lead to an adiabatic collapse, magnetic flux compression, and photon emissions reaching an Eddington limit. At this point the photon luminosity would need to support a smaller diameter and more tightly gravitationally bound mass. A new photon Eddington balance would thus require an escaping luminosity reduced by at least the $\sim 10^{20}$ opacity ratio (σ_T/σ_ν), where $\sigma_T = 6.6 \times 10^{-25}$ cm² is the Thompson cross section and $\sigma_\nu = 4.4 \times 10^{-45}$ cm² is the neutrino scattering cross-section. Thus $L_\infty \lesssim 10^{31-32}$ erg/s would be required. For this to be $L_{edd,\infty}$ for a 10 M_\odot GBHC would require $1+z \sim 10^8$. The adiabatic relaxation of neutrino support and formation of a pair plasma is an important step in gravitational collapse that is not encompassed by polytropic equation of state models of collapse. It is of some interest that if neutrinos have non-zero rest mass they might be trapped inside the photon sphere anyway.

for large z . (See Appendix A). Here we have used

$$\frac{R_g}{R} = \frac{1}{2} \left(1 - \frac{1}{(1+z)^2}\right) \quad (26)$$

where R and z refer to the location from which photons escape. The net outflow fraction of the luminosity provides the support for the collapsing matter, thereby dynamically maintaining the SPOE requirement of timelike world line completeness. The photons which finally escape do so from the photosphere of the pair atmosphere. The fraction of luminosity from the MECO surface that escapes to infinity in Eddington balance is

$$(L_{edd})_s = \frac{4\pi GM_s c(1+z)}{\kappa} = 1.27 \times 10^{38} m(1+z_s) \text{ erg/s} \quad (27)$$

The distantly observed luminosity is:

$$L_\infty = \frac{(L_{edd})_s}{(1+z_s)^2} = \frac{4\pi GM_s c}{\kappa(1+z_s)} \quad (28)$$

When radiation reaches the photosphere, where the temperature is T_p , the fraction that escapes to be distantly observed is:

$$L_\infty = \frac{4\pi R_g^2 \sigma T_p^4 27}{(1+z_p)^4} = 1.56 \times 10^7 m^2 T_p^4 \frac{27}{(1+z_p)^4} \text{ erg/s} \quad (29)$$

where $\sigma = 5.67 \times 10^{-5}$ erg/s/cm² and subscript p refers to conditions at the photosphere. Equations 28 and 29 yield:

$$T_\infty = T_p/(1+z_p) = \frac{2.3 \times 10^7}{(m(1+z_s))^{1/4}} \text{ K}. \quad (30)$$

To examine typical cases, a $10M_\odot$, $m = 10$ GBHC modeled in terms of a MECO with $z \sim 10^8$ would have $T_\infty = 1.3 \times 10^5 K = 0.01$ keV, a bolometric luminosity, excluding spin-down contributions, of $L_\infty = 1.3 \times 10^{31}$ erg/s, and a spectral peak at 220 Å⁰, in the photoelectrically absorbed deep UV. For an $m=10^7$ AGN, $T_\infty = 4160K$, $L_\infty = 1.3 \times 10^{37}$ erg/s and a spectral peak in the near infrared at 7000 Å^o. (Sgr A* at $m \approx 3 \times 10^6$, would have $T_\infty = 5500$ K, and a 2.2 micron brightness of 6 mJy, just below the observational upper limit of 9 mJy (Reid et al. 2003).) Hence passive MECO without active accretion disks, although not black holes, have lifetimes much greater than a Hubble time and emit highly red shifted quiescent thermal spectra that may be quite difficult to observe. There are additional power law components of similar magnitude that originate as magnetic dipole spin-down radiation (see below).

Escaping radiation passes through a pair plasma atmosphere that can be shown, *ex post facto* (See Appendix B), to be radiation dominated throughout. Under these circumstances, the radiation pressure within the equilibrium

atmosphere obeys $P_{rad}/(1+z) = constant$.⁷ Thus the relation between surface and photosphere temperatures is $T_s^4/(1+z_s) = T_p^4/(1+z_p)$. At the MECO surface, we expect a pair plasma temperature of $T_s \approx m_e c^2/k \sim 6 \times 10^9 K$ because an equipartition magnetic field effectively acts as a thermostat which buffers the temperature of the optically thick synchrotron radiation escaping from the MECO surface (Pelletier & Marcowith 1998). But since $T_\infty = T_p/(1+z_p)$, we have that

$$T_p = T_s \left(\frac{T_s}{T_\infty(1+z_s)} \right)^{1/3} = 1.76 \times 10^9 \left(\frac{m}{1+z_s} \right)^{1/12} K \quad (31)$$

For a $m = 10$ and $1+z_s = 10^8$ GBHC, this yields a photosphere temperature of $4.6 \times 10^8 K$, from which $(1+z_p) = 3500$. An AGN with $m = 10^7$ would have a somewhat warmer photosphere at $T_p = 1.5 \times 10^9 K$, but with a red shift of 360000.

7. AN ACTIVELY ACCRETING MECO

From the viewpoint of a distant observer, accretion would deliver mass-energy to the MECO, which would then radiate most of it away. The contribution from the central MECO alone would be

$$L_\infty = \frac{4\pi GM_s c}{\kappa(1+z_s)} + \frac{\dot{m}_\infty c^2}{1+z_s} (e(1+z_s)-1) = 4\pi R_g^2 \sigma T_p^4 \frac{27}{(1+z_p)^4} \quad (32)$$

where $e = E/mc^2 = 0.943$ is the specific energy per particle available after accretion disk flow to the marginally stable orbit radius, r_{ms} . Assuming that \dot{m}_∞ is some fraction, f , of the Newtonian Eddington limit mass accretion rate, $4\pi GMc/\kappa$, then

$$1.27 \times 10^{38} \frac{m\eta}{1+z_s} = (27)(1.56 \times 10^7) m^2 \left(\frac{T_p}{1+z_p} \right)^4 \quad (33)$$

where $\eta = 1 + f((1+z_s)e - 1)$ includes both quiescent and accretion contributions to the luminosity. Due to the extremely strong dependence on temperature of the density of pairs, (see Appendix B) it is unlikely that the temperature of the photosphere will be greatly different from the average of $4.6 \times 10^8 K$ found previously for a typical GBHC. Assuming this to be the case, along with $z = 10^8$, $m = 10$, and $f = 1$, we find $T_\infty = T_p/(1+z_p) = 1.3 \times 10^7 K$ and $(1+z) = 35$, which indicates considerable photospheric expansion. The MECO luminosity would be approximately Newtonian Eddington limit at $L_\infty = 1.2 \times 10^{39}$ erg/s. For comparison, the accretion disk outside the marginally stable orbit at r_{ms} (efficiency = 0.057) would produce only 6.8×10^{37} erg/s. Thus the high accretion state luminosity of a GBHC would originate primarily from the central MECO. The thermal component would be ‘ultrasoft’ with a temperature of only $1.3 \times 10^7 K$ (1.1 keV). A substantial fraction of the softer thermal luminosity would be Compton scattered to higher energy in the plunging flow inside r_{ms} . Even if a disk flow could be maintained all the way to the MECO surface, where a hot equatorial band might result, the escaping radiation would be spread over the

larger area of the photosphere due to photons origins deep inside the photon orbit.

For radiation passing through the photosphere most photons would depart with some azimuthal momentum on spiral trajectories that would eventually take them across and through the accretion disk. Thus a very large fraction of the soft photons would be subject to bulk comptonization in the plunging region inside r_{ms} . This contrasts sharply with the situation for neutron stars where there probably is no comparable plunging region and few photons from the surface cross the disk. This could account for the fact that hard x-ray spectral tails are comparatively much stronger for high state GBHC. Our preliminary calculations for photon trajectories randomly directed upon leaving the photon sphere indicate that this process would produce a power law component with photon index greater than 2. These are difficult, but important calculations for which the effects of multiple scattering must be considered. But they are beyond the scope of this paper, which is intended as a first description of the general MECO model.

8. SPECTRAL STATES

The progression of configurations of accretion disk, magnetic field and boundary layer is shown in Figure 1. The caption summarizes the spectral features expected in four regimes:

Quiescence

A low accretion rate is ablated by $\sim 10^{30-33}$ erg/s radiation from the central object at a large inner disk radius. This luminosity is sufficient to raise the temperature of the optically thick inner disk above the $\sim 5000 K$ instability temperature for hydrogen out to a distance of $r \sim 10^{10}$ cm. Therefore we expect the quiescent inner disk to be essentially empty with a large inner radius. The rate of mass flow ablated at the inner disk radius would only need to be $\sim 10^{13}$ g/s to produce the quiescent optical emission observed for GBHC and NS. The ablated material could escape if it reached the magnetic propeller region, which is confined to the light cylinder at a much smaller radius, r_{lc} , than that of the inner disk. This makes the MECO model compatible with the disk instability model of x-ray nova outbursts, which begin as ‘outside-in’ events in which substantial outer mass reservoirs have been observed to fill an accretion disk on the viscous timescale of a very subsonic radial flow (Orosz et al. 1997).

Quiescent luminosities that are generally 10 - 100 X lower for GBHC than for neutron stars (NS) have been claimed as evidence for the existence of event horizons. (Narayan et al. 1997, Garcia et al. 2001). In the MECO model, the quiescent emissions are magnetic dipole emissions that are characteristic of the magnetic moment and rate of spin of the central object. The lower quiescent luminosities of the GBHC are explained by their lower spin rates and (perhaps unobservably) low rates of quiescent emission from the central MECO.

Low State

The inner disk radius is inside the light cylinder, with hot, diamagnetic plasma reshaping the magnetopause topology (Arons et al. 1984). This magnetic propeller regime (Har-

⁷Due to its negligible mass, we consider the pair atmosphere to exist external to the Meco. Due to the slow collapse, the exterior Vaidya metric can be approximated by exterior, outgoing Finkelstein coordinates. In this case, the hydrostatic balance equation within the MECO atmosphere is $\frac{\partial p}{\partial r} = -\frac{\partial \ln(g_{00})}{2\partial r} (p + \rho c^2)$, where $g_{00} = (1 - 2R_g/r)$ and $\rho c^2 \ll p$. This integrates to $p/(1+z) = constant$.

ianov & Sunyaev 1975, Stella, White & Rosner 1986, Cui 1997, Zhang, Yu & Zhang 1997, Campana et al. 1998) exists until the inner disk pushes inside the co-rotation radius, r_c . At that time, large fractions of the accreting plasma can continue on to the central object and produce a spectral state switch to softer emissions. In previous work (Robertson & Leiter 2002) we found that magnetic moments and spin rates could be determined from luminosities at the end points of the spectral hardening transition. The magnetic moments and spins were used to calculate the $\sim 10^3$ – 10^6 times fainter quiescent luminosities expected from spin-down. The results are recapitulated and extended in Table 1 and Appendix D. Calculated values of quiescent luminosity in Table 1 have been corrected using a more recent correlation of spin-down energy loss rate and soft x-ray luminosity (Possenti et al. 2002), but results are otherwise unchanged from the previous work except for new additions listed in bold font. It is very powerful confirmation of the propeller mechanism that spins are in good agreement with burst oscillation frequencies (Strohmayer & Markwart 2002, Chakrabarty et al. 2003), magnetic moments are of similar magnitude to those determined from the spin-down of similarly rotating millisecond pulsars and the calculated quiescent luminosities are accurate.

Plasma flowing outward in the low state may depart in a jet, or as an outflow back over the disk as plasma is accelerated on outwardly curved or open magnetic field lines. Radio images of both flows have been seen (Paragi et al. 2002). Equatorial outflows could contribute to the low state hard spectrum by bulk Comptonization of soft photons in the outflow. This would accentuate the hardness by the depletion of the soft photons that would otherwise be observed to arise from the disk. Such an outflow would be compatible with partial covering models for dipping sources, in which the hard spectral region seems to be extended (Church 2001, Church & Balucinska-Church 2001). Alternatively, an accretion disk corona or compact jet might be a major contributor to the hard spectrum. For jet emissions, recent work (Corbel & Fender 2002) has shown that it may be possible to explain much of the broadband emissions from near infrared through soft x-rays as the power-law synchrotron emissions of compact jets, which have been directly imaged for some GBHC.

Intermediate State

Intermediate states occur when some, but not all, of the accreting matter can make its way to the central object. Incomplete spectral state switches terminating well below the Eddington limit, such as those exhibited by Cygnus X-1 may occur. If the co-rotation radius is large, there is a very large difference in the efficiency of energy release at the central object vs the disk. Thus changes of luminosity and an apparent spectral state switch can occur for very small change of accretion rate. Relaxation oscillations driven by intermittent radiation from the central object can occur if the accretion rate is not steady. Large periodic jet ejections may be associated with this state, for which significant toroidal winding of the poloidal magnetic field lines and radiation pressure may contribute to the ejection (see below).

High State

With the disk inner radius inside r_c , the propeller regime ends and matter of sufficient pressure can make its way

inward. From quiescence to the light cylinder, the x-ray luminosity changes by a factor of only a few as the disk generates a soft thermal spectral component (which may be mistaken for surface radiation for NS.) From r_{lc} to r_c , the x-ray luminosity may increase by a factor of $\sim 10^3$ – 10^6 . With inner disk inside r_c , the outflow and/or jets subside, the system becomes radio quiet, the photon index increases, and a soft thermal excess from the central object appears, both of which contribute to a softer spectrum, (e.g., see Fig. 3.3 of Tanaka & Lewin, p. 140), which may be even be described as ‘ultrasoft’ (White & Marshall 1984); particularly when the central object cools as the luminosity finally begins to decline. We have shown that MECO would produce a dominant ‘ultrasoft’ component in the high state. They would also produce an extensive power-law hard tail as soft photons leaving the MECO well inside the photon orbit take trajectories that take them across the plunging region inside the marginally stable orbit. Since there is no comparably rich source of photons on disk crossing trajectories for NS and a much smaller, if any, plunging region, there is no comparable hard spectral component in their high states. Another mechanism that might contribute to the power-law tail is cyclotron resonance scattering in the outer photosphere (Thompson, Lyutikov & Kulkarni 2002). In either case, the high state hard tail has different origins and characteristics from the hard tail of the low state.

9. DISK CHARACTERISTICS

For matter sufficiently inside r_c , the propeller mechanism is incapable of stopping the flow, however, a boundary layer may form at the inner disk radius in this case. The need for a boundary layer for GBHC can be seen by comparing the magnetic pressure at the magnetosphere with the impact pressure of a trailing, subsonic disk. For example, for an average GBHC magnetic moment of $\sim 4 \times 10^{29}$ gauss cm³ from Table 1, the magnetic pressure at a r_{ms} radius of 6.3×10^6 cm for a $7 M_\odot$ GBHC would be $B^2/8\pi \sim 10^{17}$ erg/cm³. At a mass flow rate of $\dot{m} = 10^{18}$ g/s, which would be near Eddington limit conditions for a $7 M_\odot$ MECO, the inner disk temperature would be $T \sim 1.5 \times 10^7$ K. The disk scale height would be given by $H \sim rv_s/v_K \sim 0.0036r$, where $v_s \sim 4.5 \times 10^7$ cm/s and $v_K \sim 1.2 \times 10^{10}$ cm/s are acoustic and Keplerian speeds, respectively. The impact pressure would be $\dot{m}v_r/4\pi rH \sim 5.6 \times 10^5 v_r$ erg/cm³. It would require v_r in excess of the speed of light to let the impact pressure match the magnetic pressure. But since the magnetic field doesn’t eject the disk material inside r_c , matter piles up as essentially dead weight against the magnetopause and pushes it in. The radial extent of such a layer would only need to be $\sim kT/m_p g \sim 50$ cm, where m_p is the proton mass and g , the radial gravitational free fall acceleration, but it is likely distributed over a larger transition zone from co-rotation with the magnetosphere to Keplerian flow. The gas pressure at the inner radius of the transition zone necessarily matches the magnetic pressure. In this case, radiation pressure in the disk, at $T = 1.5 \times 10^7$ K, is nearly three orders of magnitude below the gas pressure. Therefore a gas pressure dominated, thin, Keplerian disk with subsonic radial speed should continue all the way to r_{ms} for a MECO. Similar conditions occur with disk radius inside r_c even for weakly magnetic

TABLE 1
^aCALCULATED AND OBSERVED QUIESCENT LUMINOSITIES

Object	m M _⊙	L_{min} 10 ³⁶ erg/s	L_c 10 ³⁶ erg/s	μ_{27} Gauss cm ³	ν_{obs} Hz obs.	ν_{calc} Hz calc.	log (L_q) erg/s obs.	log (L_q) erg/s calc.
NS								
Aql X-1	1.4	1.2	0.4	0.47	549	658	32.6	32.5
4U 1608-52	1.4	10	2.9	1.0	619	534	33.3	33.4
Sax J1808.4-3658	1.4	^b 0.8	0.2	0.53	401	426	31.8-32.2	32
Cen X-4	1.4	4.4	1.1	1.1		430	32.4	32.8
KS 1731-26	1.4		1.8	1.0	524		^c 32.8	33.1
XTE J1751-305	1.4		3.5	1.9	435		<34.3	33.7
XTE J0929-314	1.4		4.9	8.5	185			33.1
4U 1916-053	1.4	~14	3.2	3.7	270	370		33.0
4U1705-44	1.4	26	7	2.5		470		33.7
4U 1730-335	1.4	10		2.5	307			32.9
GRO J1744-28	1.4		18	13000	2.14			31.5
Cir X-1	1.4	300	14	170		35		32.8
GBHC								
GRS 1124-68	5	240	6.6	720		16	< 32.4	32.7
GS 2023+338	7	1000	48	470		46	33.7	34
XTE J1550-564	7	^d 90	4.1	150		45	32.8	32.2
GS 2000+25	7		0.15	160		14	30.4	30.5
GRO J1655-40	7	31	1.0	250		19	31.3	31.7
A0620-00	4.9	4.5	0.14	50		26	30.5	30.2
Cygnus X-1	10		30	1260		23		33
GRS 1915+105	7		12	130	^e 67			33
XTE J1118+480	7		1.2	1000		8		31.5
LMC X-3	7	600	7	860		16		33

^aNew table entries in bold font are described in Appendix D.

Equations used for calculations of spins, magnetic moments and L_q are in Appendix D.

Other tabular entries and supporting data are in Robertson & Leiter (2002)

^b2.5 kpc, ^c (Burderi et al. 2002), ^dd = 4 kpc

^eGRS 1915+105 Q ≈ 20 QPO was stable for six months and a factor of five luminosity change.

‘atoll’ class NS. The similar magnetic pressures at r_c for GBHC and atolls is one of the reasons for their spectral and timing similarities. The nature of mass accumulations in the inner disk transition region and the way that they can enter the magnetosphere have been the subject of many studies, (e.g., Spruit & Taam 1990).

In the case of NS, sufficiently high mass accretion rates can push the magnetopause into the star surface, but this requires near Eddington limit conditions. At this point the hard apex of the right side of the horizontal branch of the ‘Z’ track in the hardness/luminosity diagram is reached. It has recently been shown (Muno et al. 2002) that the distinction between ‘atoll’ and ‘Z’ sources is merely that this point is reached near the Eddington limit for ‘Zs’ and at perhaps $\sim 10 - 20\%$ of this luminosity (Barrett & Olive 2002) for the less strongly magnetized ‘atolls’. Atolls rarely reach such luminosities. For MECO based GBHC, one would expect a relatively constant ratio of hard and soft x-ray ‘colors’ after the inner disk crosses r_c and the flow reaches the photon orbit. If x-ray ‘color’ bands for GBHC were chosen below and above a $\sim 1keV$ thermal peak similarly to way they are now chosen to bracket the $\sim 2keV$ peak of NS, one might observe a ‘Z’ track for the color/color diagrams of GBHC.

An observer at coordinate, r , inside r_{ms} , would find the radial infall speed to be $v_r = \frac{\sqrt{2}}{4}c(6R_g/r - 1)^{3/2}$, (see Appendix A) and the Lorentz factor for a particle spiraling in from $6R_g$ would be $\gamma = 4\sqrt{2}(1+z)/3$, where $1+z = (1 - 2R_g/r)^{-1/2}$ would be the red shift for photons generated at r . If the distantly observed mass accretion rate would be \dot{m}_∞ , then the impact pressure at r would be $p_i = (1+z)\dot{m}_\infty\gamma v_r/(4\pi rH)$. For $\dot{m}_\infty \sim 10^{18}$ g/s, corresponding to Eddington limit conditions for a $7 M_\odot$ GBHC, and $H = 0.0036r$, impact pressure is, $p_i \sim 5 \times 10^{16}(1+z)^2(2R_g/r)^2(6R_g/r - 1)^{3/2}$ erg/cm³. For comparison, the magnetic pressure is $(1+z)^2 B_\infty^2/8\pi$. Assuming a dipole field with average magnetic moment of 4×10^{29} gauss cm³ from Table 1, the magnetic pressure is $\sim 10^{20}(1+z)^2(2R_g/r)^6$ erg/cm³. Thus there are no circumstances for which the impact pressure is as large as the magnetic pressure for $2R_g < r < 6R_g$. We conclude that another weighty boundary layer must form inside r_{ms} if the magnetosphere is to be pushed inward. More likely, the plasma stream is broken up by Kelvin-Helmholtz instabilities and filters through the magnetosphere. In any event, the inner radius of the disk is determined by the rate at which the magnetic field can strip matter and angular momentum from the disk. This occurs in a boundary layer of some thickness, δr , that is only a few times the disk thickness. (See Appendix C)

Other than the presence of a transition boundary layer on the magnetopause, the nature of the flow and spectral formation inside r_c is a research topic. Both the short radial distance from r_c to r_{ms} and the magnetopause topology should help to maintain a disk-like flow to r_{ms} . Radial acceleration inside r_{ms} should also help to maintain a thin flow structure. These flows are depicted in Figure 1. Recapitulating, we expect the flow into the MECO to produce a distantly observed soft thermal component, part of which is strongly bulk Comptonized.

Quasi-periodic Oscillations

Although many mechanisms have been proposed for the

high frequency quasi-periodic oscillations (QPO) of x-ray luminosity, they often require conditions that are incompatible with thin, viscous Keplerian disks. Several models have requirements for lumpy flows, elliptical inner disk boundaries, orbits out of the disk plane or conditions that should produce little radiated power. In a conventional thin disk, the vertical oscillation frequency, which is approximately the same as the Keplerian frequency of the inner viscous disk radius should generate ample power. Accreting plasma should periodically wind the poloidal MECO magnetic field into toroidal configurations until the field lines break and reconnect across the disk. Field reconnection across the disk should produce high frequency oscillations that couple to the vertical oscillations. If so, there would be an automatic association of high frequency QPO with the harder power-law spectra of magnetospherically driven emissions, as is observed. Mass ejection in low state jets might be related to the heating of plasma via the field breakage mechanism, in addition to natural buoyancy of a plasma magnetic torus in a poloidal external field.

It seems possible that toroidal winding and reconnection of field lines at the magnetopause, might continue in high states inside r_{ms} . If so, there might be QPO that could be identified as signatures of the MECO magnetosphere. If they occur deep within the magnetosphere, they might be at locally very high frequencies, and be observed distantly as very redshifted low frequencies. As shown in Appendix A, the ‘Keplerian’ frequencies in the plunging region inside r_{ms} are given by $\nu = 1.18 \times 10^5 (R_g/r)^2 (1 - 2R_g/r)/m$ Hz. A maximum frequency of 437 Hz would occur for $m=10$ at the photon orbit. Of more interest, however are frequencies for $R_g/r \approx 1/2$, for which $\nu = 2950/(m(1+z)^2)$ Hz. For $1+z = 10 - 100$, $m = 10$; conditions that might apply to the photosphere region, $\nu \sim 0.03 - 3$ Hz could be produced. In this regard, one could expect significant time lags between inner disk accretion and luminosity fluctuations and their echoes from the central highly redshifted MECO.

Even if QPO are not produced inside r_{ms} or inside the photon sphere for GBHC, there is an interesting scaling mismatch that might allow them to occur for AGN. Although the magnetic moments of AGN scale inversely with mass, the velocity of plasma inside r_{ms} does not. Thus the energy density of disk plasma inside r_{ms} will be relatively larger than magnetic field energy densities for AGN accretion disks. When field energy density is larger than kinetic energy density of matter, the field pushes matter around. When the reverse is true, the matter drags the field along. Thus toroidal winding of the field at the magnetopause could fail to occur for GBHC, but might easily do so for AGN. If the process is related to mass ejection, then very energetic jets with Lorentz factors $\gamma \sim (1+z)$ might arise from within r_{ms} for AGN. A field line breakage model of ‘smoke ring’ like mass ejection from deep within r_{ms} has been developed by Chou & Tajima (1999). In their calculations, a pressure of unspecified origin was needed to stop the flow outside $2R_g$ and a poloidal magnetic field, also of unspecified origin was required. MECO provide the necessary ingredients in the form of the intrinsic MECO magnetic field. The Chou & Tajima mechanism, aided by intense radiation pressure, may be active inside r_{ms} for GBHC and produce extremely large episodic mass ejection.

tions such as those shown by GRS 1915+105. Although not developed for conditions with large inner disk radius, the same magnetic mechanism could produce the jet emissions associated with the low/hard state (Gallo, Fender & Pooley 2003).

Finally, some of the rich oscillatory behavior of GRS 1915+105 may be readily explained by the interaction of the inner disk and the central MECO. The objects in Table 1 have co-rotation radii of order $20R_g$, which brings the low state inner disk radius in close to the central object. A low state MECO, balanced near co-rotation would need only a small increase of mass flow rate to permit mass to flow on to the central MECO. This would produce more than 20X additional luminosity and enough radiation pressure to blow the inner disk back beyond r_c and load its mass onto the magnetic field lines where it is ejected. This also explains the association of jet outflows with the oscillatory states. Belloni et al. (1997) have shown that after ejection of the inner disk, it then refills on a viscous time scale until the process repeats. Thus one of the most enigmatic GBHC might be understood as a relaxation oscillator, for which the frequency is set by a critical mass accretion rate.

10. DETECTING MECO

It may be possible to detect MECO in several ways. Firstly, as we have shown, for a red shift of $z \sim 10^8$, the quiescent luminosity of a GBHC MECO would be $\sim 10^{31}$ erg/s with $T_\infty \sim 0.01$ keV. This thermal peak might be observable for nearby or high galactic latitude GBHC, such as A0620-00 or XTE J1118+480. Secondly, at moderate luminosities $L \sim 10^{36} - 10^{37}$ erg/s but in a high state at least slightly above L_c , a central MECO would be a bright, small central object that might be sharply eclipsed in deep dipping sources. A high state MECO should stand out as a small bright source. This is consistent with analyses of absorption dips in GRO J1655-40 (Church 2001) which have shown the soft source of the high state to be smaller than the region that produces the hard spectral component of its low states. A conclusive demonstration that most of the soft x-ray luminosity of a high state GBHC is distributed over a large accretion disk would be inconsistent with MECO or any other GBHC model entailing a central bright source. If the MECO model is correct, the usual identification of the bright, high state soft component as disk emissions would be wrong. Thirdly, a pair plasma atmosphere in an equipartition magnetic field should be virtually transparent to photon polarizations perpendicular to the magnetic field lines. The x-rays from the central MECO should exhibit some polarization that might be detectable, though this is far from certain since the distantly observed emissions could originate from nearly any point on the photosphere. MECO presumably would not be found only in binary systems. If they are the offspring of massive star supernovae, then they should be found all over the galaxy. If we have correctly estimated their quiescent temperatures, isolated MECO would be weak, possibly polarized, EUV sources with a power-law tail in soft

x-rays.

11. CONCLUSIONS

It is now becoming apparent that many of the spectral properties of LMXB, including the GBHC, are consistent with the existence of intrinsically magnetized central objects. We have shown that the existence of intrinsically magnetic GBHC are consistent with a new class of magnetospheric eternally collapsing object (MECO) solutions of the Einstein field equations of General Relativity. These solutions are based on a strict adherence to the Strong Principle of Equivalence (SPOE) requirement for timelike world line completeness; i.e., that the world lines of physical matter under the influence of gravitational and non-gravitational forces must remain timelike in all regions of spacetime. Since there is nothing in the structure of the Einstein tensor, $G^{\mu\nu}$, on the left hand side of the Einstein field equation that dynamically enforces ‘time like world line completeness’, we have argued that the SPOE constrains the physically acceptable choices of the energy momentum tensor, $T^{\mu\nu}$ to contain non-gravitational forces that can dynamically enforce it. In this context we have found the MECO solutions. Since MECO lifetimes are orders of magnitude greater than a Hubble time, they provide an elegant and unified framework for understanding the broad range of observations associated with GBHC and active galactic nuclei.

An enormous body of physics scholarship developed primarily over the last half century has been built on the assumption that trapped surfaces leading to event horizons and curvature singularities exist. Misner, Thorne & Wheeler (1973), for example in Sec. 34.6 clearly state that this is an assumption and that it underlies the well-known singularity theorems of Hawking and Penrose. In contrast, we have found that strict adherence to the SPOE demand for timelike world line completeness requires a ‘*no trapped surface condition*’. This has led to the quasi-stable, high red shift MECO solutions of the Einstein field equations. The physical mechanism of their stable rate collapse is an Eddington balance maintained by the distributed photon generation of an equipartition magnetic field. This field also serves to confine the pair plasma dominated outer layers of the MECO and the thin MECO pair atmosphere. Red shifts of $z \sim 10^8$ have been found to be necessary for compatibility with our previously found magnetic moments for GBHC.

We have delineated the expected spectral properties of MECO in quiescence and in accreting states and shown that the central magnetic moments are large enough to require their accretion disks to be dominated by gas pressure, though the inner disk may be subject to substantial irradiation. The MECO model seems able to robustly account for the general spectral and timing behaviours of GBHC while providing for their appropriate quantitative differences from NS. Lastly, we have indicated some ways in which MECO might be detected and confirmed.

REFERENCES

- Abramowicz, M., Kluzniak, W. & Lasota, J-P, 2002 A&A 396, L31
 Abrams, L. S., 1979 Phys. Rev. D 20, 2474
 Abrams, L. S., 1989 Can J. Phys. 67, 919, gr-qc/0102051
 Arons, J. et al. 1984 in ‘High Energy Transients in Astrophysics’, AIP Conf. Proc. 115, 215, Ed. S. Woosley, Santa Cruz, CA
 Barret, D. & Olive, J-F., 2002 ApJ 576, 391

- Belloni, T., Mendez, M., King, A., van der Klis, M. & van Paradijs, J. 1997 ApJ 488, L109
- Baumgarte, T. & Shapiro, S. 2003 ApJ 585, 930
- Bhattacharya D., & Srinivasan, G., 1995 in 'X-Ray Binaries', eds W. Lewin, J. van Paradijs & E. van den Heuvel, Cambridge Univ. Press
- Bisnovatyi-Kogan, G. & Lovelace, R. 2000 APJ 529, 978
- Boyd, P. et al. 2000 ApJ 542, L127
- Burderi, L., et al. 2002 ApJ 574, 930
- Campana, S. et al., 2002 ApJ 580, 389
- Campana, S. et al., 1998 A&A Rev. 8, 279
- Chakrabarty, D. et al., 2003 Nature 424, 42
- Chou & Tajima 1999 ApJ 513, 401
- Church, M.J. 2001 in Advances in Space Research, 33rd Cospar Scientific Assembly, Warsaw, Poland July 2000 astro-ph/0012411
- Church, M. & Balucinska-Church, M. 2001 A&A 369, 915
- Coburn, W. & Boggs, S., 2003 Nature 423, 415
- Corbel, S. & Fender, R. 2002 ApJ 573, L35
- Cui, W. 1997 ApJ 482, L163
- Done, C. & Życki, P. 1999 MNRAS 305, 457
- Gallo, E., Fender, R. & Pooley, G., 2003 MNRAS, in press astro-ph/0305231
- Galloway, D., Chakrabarty, D., Morgan, E., & Remillard, R. 2002 ApJL 576, 137
- Garcia, M. et al. 2001 ApJ 553, L47
- Gliozzi, M., Bodo, G. & Ghisellini, G. 1999 MNRAS 303, L37
- Gnedin, Y. et al., 2003 Astrophys. Sp. Sci accepted, astro-ph/0304158
- Goodson, A., Bohm, K. & Winglee, R. 1999 ApJ 534, 142
- Haensel, P. & Bonazzola, S., 1996 A & A, 314, 1017, and references cited therein.
- Hawley, J., Balbus, S. & Winters, W., 1999 ApJ 518, 394
- Hernandez Jr., W.C. & Misner, C.W., 1966 ApJ. 143, 452
- Iaria, R. et al. 2001 ApJ 547, 412
- Ibrahim, A., Swank, J. & Parke, W., 2003 ApJ 584, L17
- Ilarianov, A. & Sunyaev, R. 1975 A&A 39, 185
- Kippenhahn, R. & Weigert, A. 1990 'Stellar Structure and Evolution' Springer-Verlag, Berlin Heidelberg New York
- Kluzniak, W. & Ruderman, M., 1998 ApJL 505, 113
- Landau, L.D. & Lifshitz, E. M., 1975 'Classical Theory of Fields', 4th Ed, Pergamon Press p248-252
- Landau, L. & Lifshitz, E. 1958 'Statistical Physics', Pergamon Press LTD, London
- Leiter, D. & Robertson, S., 2003 Found Phys. Lett. 16 143
- Lindquist, R. W., Schwartz, R. A. & Misner, C. W. 1965 Phys. Rev., 137B, 1364.
- Lindquist, R. W., 1966 Annals of Physics, 37, 487
- Livio, M., Ogilvie, G. & Pringle, J. 1999 ApJ 512, 100
- Markoff, S., Falcke H., & Fender, R. 2001 A&AL 372, 25
- Markwardt, C., et al. 2002 ApJL 575, 21
- Mauche, C. W., 2002 ApJ 580,423
- McClintock, J. et al., 2001 ApJ 556, 42
- Miller, J. et al., 2003 ApJL, 583, 99
- Misner, C. W. 1965 Phys. Rev., 137B, 1360
- Misner, C., Thorne, K. & Wheeler, J. 1973 'Gravitation', Freeman, San Francisco, California
- Mitra, A. 2000 Found. Phys. Lett. 13, 543
- Mitra, A., 2002 Found. Phys. Lett. 15, 439
- Muno, M., Remillard, R. & Chakrabarty, D. 2002 ApJ 568, L35
- Narayan, R., Garcia, M., McClintock, J., 1997 ApJ. 478, L79
- Orosz, J., Remillard, R., Bailyn, C. & McClintock, J. 1997 ApJ 478, L83
- Paragi, Z., et al. 2002 Talk presented at the 4th Microquasar Workshop, Cargese, Corsica May 27-31 astro-ph/0208125
- Pelletier, G. & Marcowith, A., 1998 ApJ 502, 598
- Possenti, A., Cerutti, R., Colpi, M., & Mereghetti, S. 2002 A&A 387, 993
- Punsly, B. 1998 ApJ 498, 640
- Reid, M. et al., 2003 ApJ 587, 208
- Rindler, W. 1977, 'Essential Relativity, 2nd Ed. Springer-Verlag, New York, Berlin, Heidelberg
- Robertson, S. & Leiter, D. 2002 ApJ, 565, 447
- Shapiro, S. & Teukolsky, S. 1983 in 'Black Holes, White Dwarfs & Neutron Stars', John Wiley & Sons, Inc., New York
- Soria, R., Page, M. & Wu, K. 2002 in Proceedings of the Symposium 'New Visions of the X-Ray Universe in the XMM-Newton & Chandra Era', Nov. 2001, ESTEC, the Netherlands, astro-ph/0202015
- Spruit, H. & Taam, R. 1990 A&A 229, 475
- Stella, L., White, N. & Rosner, R. 1986 ApJ 308, 669
- Strohmayer, T. & Markwardt, C., 2002 ApJ 577, 337
- Tanaka, Y. & Lewin, W., 1995 in 'Black-hole binaries' in X-ray Binaries ed. W. Lewin, J. van Paradijs & E. van den Heuvel (Cambridge: Cambridge Univ. Press)
- Tanaka, Y. & Shibasaki, N., 1996 ARA&A, 34, 607
- Tatsumi, T., 2000 astro-ph/0004062
- Thompson, C., Lyutikov, M. & Kulkarni, S. 2002 ApJ 574, 332
- Thorne, K., 1965 Phys. Rev. 138, B251
- Thorne, K., 1994 in 'Black Holes And Time Warps', p263, John Wiley & Sons, Inc., New York
- Titarchuk, L. & Wood, K., 2002 ApJL 577, 23
- Vadawale, S., Rao, A. & Chakrabarti, S. 2001 A&A 372, 793V
- van der Klis, M. 1994 ApJS 92, 511
- Warner, B. & Woudt, P., 2003 in ASP Conf. Series, Ed. M. Cuppi and S. Vriellmann astro-ph/0301168
- Weinberg, S. 1972 'Gravitation and Cosmology', John Wiley & Sons, Inc., New York
- Wheeler, J. & Ciufolini, I., 1995 in 'Gravitation And Inertia' Princeton Univ. Press, 41 William St., Princeton, New Jersey
- White, N. & Marshall, F. 1984, ApJ. 281, 354
- Wilson, C. & Done, C. 2001 MNRAS 325, 167
- Zhang, W., Yu, W. & Zhang, S. 1998 ApJ 494, L71
- Życki, P., Done, C. and Smith, D. 1997a in AIP Conf. Proc. 431, Accretion Processes in Astrophysical Systems: Some Like It Hot, Ed. S. S. Holt & T. R. Kallman (New York, AIP), 319
- Życki, P., Done, C. and Smith 1997b ApJ 488, L113

APPENDIX

A. Relativistic particle mechanics

A number of standard, but useful results for relativistic mechanics are recapitulated here. All are based upon the energy-momentum four-vector for a free particle in the singularity-free Finkelstein or Kerr-Schild coordinates for a constant central mass. Though not strictly compatible with radiating objects with variable mass, outgoing Finkelstein coordinates are a useful first order approximation to the outgoing Vaidya coordinates for low radiation rates exterior to a MECO.

$$ds^2 = dt^2((1 - 2R_g/r) \pm 4R_g v^r/r - (1 + 2R_g/r)v^r v^r) - r^2(d\theta^2 + \sin^2\theta d\phi^2) \quad (1)$$

The plus sign corresponds to outgoing Finkelstein coordinates and the negative sign to ingoing Finkelstein or Kerr-Schild coordinates. Here $v^r = dr/dt$. For a particle in an equatorial trajectory ($\theta = \pi$, $p_\theta = 0$) about an object of gravitational mass M , one obtains the same equation as for Schwarzschild coordinates:

$$\left(\frac{dr}{d\tau}\right) = -c(e^2 - (1 - 2R_g/r)(1 + a^2(R_g/r)^2))^{1/2} \quad (2)$$

Where e is the conserved energy per unit rest mass, $a = (cp_\phi/GMm_0)$ is a dimensionless, conserved angular momentum, τ is the proper time in the particle frame and the negative sign indicates movement toward $r = 0$. The metric Equation (1) also describes these radial geodesics with $ds^2 = d\tau^2$ Neglecting angular terms and letting $q = dt/d\tau$, this equation can be written as

$$1 = (1 - 2R_g/r)q^2 \pm 4pqR_g/r - (1 + 2R_g/r)p^2 \quad (3)$$

With p given above, and $a = 0$ this equation has the solution

$$q = \frac{+\sqrt{e^2} \pm 2R_g/r \sqrt{e^2 - (1 - 2R_g/r)}}{1 - 2R_g/r} \quad (4)$$

where the positive sign on the first radical has been taken to assure that time proceeds in a positive direction during the fall, and a positive second term again corresponds to outgoing coordinates. Since $v^r = p/q$, it is a straightforward matter to substitute for v^r in the original metric equation and examine the limit as $R_g/r \rightarrow 1/2$. In either ingoing or outgoing coordinates, we find that $ds^2 \rightarrow 0$ as $R_g/r \rightarrow 1/2$. Thus the radial free-fall geodesics become null upon reaching the horizon.

It is of interest, however, that in the outgoing coordinates ($+4R_g/r$) as $R_g/r \rightarrow 1/2$ one finds $v^r \rightarrow 0, q \rightarrow \infty, p \rightarrow -e$. Thus it takes an infinite coordinate time, but only a finite proper time to cross the horizon, which is the same as the well-known Schwarzschild result. In the ingoing coordinates, one obtains $v^r \rightarrow -c, q \rightarrow e, p \rightarrow -e$. In this case, only a finite coordinate time would be required to cross the horizon and coordinate speed, v^r does not change sign there. In effect, one can continue calculations through the horizon without reversing either the roles or directions of change of r and t , but at the expense of ignoring that $ds^2 = 0$ violates the SPOE requirement for timelike world line completeness. In either case, it is interesting to observe that the physical three-speed approaches that of light at the horizon (Landau & Lifshitz 1975).

$$V^2 = \left(\frac{dl}{d\tau_s}\right)^2 = c^2 \frac{(g_{0r}g_{0r} - g_{rr}g_{00})v^r v^r}{(g_{00} + g_{0r}v^r)^2} \quad (5)$$

Here we find $V \rightarrow c$ as $g_{00} \rightarrow 0$. Both the null geodesic and $V \rightarrow c$ are consequences of the vanishing of g_{00} rather than arising from a singular metric. Few would argue that the event horizon corresponding to the vanishing of g_{00} is not a surface of infinite redshift, which is what produces the null geodesic result, $d\tau = dt/(1+z) \rightarrow 0$. Finally, it should be mentioned that the vanishing of g_{00} for $r > 0$ is actually a result of a failure to apply appropriate boundary conditions for the solutions of the Einstein equations for a point mass (Abrams 1979, 1989).

For suitably small energy, bound orbits occur. Turning points for which $dr/d\tau = 0$ can be found by examining the effective potential, which consists of all terms to the right of e^2 in Equation 2. At minima of the effective potential we find circular orbits for which

$$a^2 = \frac{1}{R_g/r - 3(R_g/r)^2} \quad (6)$$

$R_g/r = 1/3$ holds at the location of an unstable circular orbit for photons (see below). From which we see that if p_ϕ is non-zero there are no trajectories for particles with both mass and angular momentum that exit from within $R_g/r = 1/3$. Thus particles with both mass and angular momentum can't escape from within the photon sphere. The minimum energy required for a circular orbit would be.

$$E = m_0 c^2 \frac{(1 - 2R_g/r)}{\sqrt{(1 - 3R_g/r)}} \quad (7)$$

In fact, however, there is an innermost marginally stable orbit for which the first two derivatives with respect to $1/r$ of the effective potential vanish. This has no Newtonian physics counterpart, and yields the well-known results: $R_g/r = 1/6$, $a^2 = 12$ and $e^2 = 8/9$ for the marginally stable orbit of radius $r_{ms} = 6GM/c^2$.

For a particle beginning a spiral descent from r_{ms} with $e = \sqrt{8/9}$, there follows:

$$\left(\frac{dr}{d\tau}\right)^2 = c^2 \frac{(6R_g/r - 1)^3}{9} \quad (8)$$

If observed by a stationary observer located at coordinate r , it would be observed to move with radial speed

$$V_r = \frac{\sqrt{2}c(6R_g/r - 1)^{3/2}}{4}. \quad (9)$$

Again, V_r approaches c as R_g/r approaches $1/2$. A distant observer would find the angular frequency of the spiral motion to be

$$\frac{1}{2\pi} \frac{d\phi}{dt} = \sqrt{9 \times 12/8} (c^3/GM) (R_g/r)^2 (1 - 2R_g/r) / 2\pi \sim 1.18 \times 10^5 (R_g/r)^2 (1 - 2R_g/r) / m \quad \text{Hz} \quad (10)$$

For a $10 M_\odot$ GBHC ($m = 10$), this has a maximum of 437 Hz and some interesting possibilities for generating many QPO frequencies, both high and low. For red shifts such that $R_g/r \approx 1/2$, the spiral frequency is $2950/(1+z)^2$ Hz.

Photon Trajectories:

The energy-momentum equation for a particle with $m_0 = 0$ can be rearranged as:

$$(1 - 2R_g/r)^2 \left(\frac{p_r GM}{p_\phi c^2}\right)^2 = \left(\frac{d(R_g/r)}{d\phi}\right)^2 = \left(\frac{GME}{p_\phi c^3}\right)^2 - (R_g/r)^2 (1 - 2R_g/r) \quad (11)$$

The right member has a maximum value of $1/27$ for $R_g/r = 1/3$. There is an unstable orbit with $d(R_g/r)/d\phi = 0$ for $R_g/r = 1/3$. To simply have $d(R_g/r)/d\phi$ be real requires $p_\phi c^3/GME < \sqrt{27}$. But $E = (1+z)pc$, where p is the entire momentum of the photon, and $1+z = (1-2R_g/r)^{-1/2}$ its red shift if it escapes to be observed at a large distance. Its azimuthal momentum component will be p_ϕ/r . Thus its escape cone is defined by:

$$\left(\frac{p_\phi}{rp}\right)^2 < 27(R_g/r)^2(1-2R_g/r) \quad (12)$$

APPENDIX

B. Pair Plasma Photosphere Conditions

Although we used a characteristic temperature of a pair plasma to locate the photosphere and find its temperature, essentially the same results can be obtained in a more conventional way. The photosphere condition is that (Kippenhahn & Weigert 1990):

$$n\sigma_T l = 2/3, \quad (1)$$

where n is the combined number density of electrons and positrons in equilibrium with a photon gas at temperature T , $\sigma_T = 6.65 \times 10^{-25} \text{cm}^2$ is the Thompson scattering cross section and l is a proper length over which the pair plasma makes the transition from opaque to transparent. Landau & Lifshitz (1958) show that

$$n = \frac{8\pi}{h^3} \int_0^\infty \frac{p^2 dp}{\exp(E/kT) + 1} \quad (2)$$

where p is the momentum of a particle, $E = \sqrt{p^2 c^2 + m_e^2 c^4}$, k is Boltzmann's constant, h is Planck's constant and m_e , the mass of an electron. For low temperatures such that $kT < m_e c^2$ this becomes:

$$n \approx 2 \left(\frac{2\pi m_e kT}{h^2} \right)^{3/2} \exp(-m_e c^2/kT) \quad (3)$$

It must be considered that the red shift may change significantly over the length l , and that $(1+z_p)$ will likely be orders of magnitude smaller than $(1+z_s)$. Neglecting algebraic signs, we can differentiate Equation (26) to obtain the coordinate length over which z changes significantly as:

$$\delta r = \frac{R_g \delta z}{(R_g/r)^2 (1+z)^3} \approx \frac{R_g}{(R_g/r)^2 (1+z)^2} \quad (4)$$

where we have taken $\delta z \approx (1+z)$. For values of z appropriate here we take $R_g/r = 1/2$. We estimate $l = \delta r(1+z) = 4R_g/(1+z)$ and replace $(1+z)$ with T/T_∞ . Substituting expressions for l and n into the photosphere condition and substituting for T_∞ from equation 30 of the main text, equation 1 yields a transcendental equation for T . For a GBHC with $z = 10^8$ and $m = 10$, its solution is $T_p = 3.3 \times 10^8 K$ and $(1+z_p) = 2500$. Then using the radiation pressure balance condition in the pair atmosphere, we find $T_s^4 = T_p^4(1+z_s)/(1+z_p)$, from which $T_s = 4.6 \times 10^9 K$. The number density of particles at the photosphere is $n = 4 \times 10^{20}$ and 10^9 times larger at the MECO surface. Nevertheless, the radiation pressure exceeds the pair particle pressure there by ten fold. This justifies our use of radiation dominated pressure in the pair atmosphere. For an AGN with $1+z = 10^8$ and $m = 10^7$, we obtain photosphere and surface temperatures of $2 \times 10^8 K$ and $1.4 \times 10^9 K$, respectively, and $(1+z_p) = 50000$. We note that the steep temperature dependence of the pair density would have allowed us to find the same photosphere temperature within a few percent for any reasonable choice of l from 10^3 to 10^6 cm. In the present circumstance, we find $l = 4R_g/(1+z) = 2.4 \times 10^4$ cm. This illustrates the extreme curvature of spacetime as the corresponding coordinate interval thickness of the pair atmosphere for the distant observer is only $\delta r \sim 10$ cm.

APPENDIX

C. Magnetosphere - Disk Interaction

We have found the inner accretion disk of MECO to be gas pressure dominated. Impact pressure is not sufficient to push the magnetosphere inward. The frequently used balance of impact and magnetic pressures to determine the inner radius of the disk is not applicable. What is required instead is that the stagnation pressure match the magnetic stress. Here we show that the same inner radius scaling is obtained by merely requiring that the magnetosphere remove disk angular momentum at an appropriate rate. The torque per unit volume of plasma in the disk threaded by magnetic field is given by $r \frac{B_z}{4\pi} \frac{\partial B_\phi}{\partial z} \sim r \frac{B_z B_\phi}{4\pi H}$, where H is the disk half thickness. Thus the rate at which angular momentum would be removed from the disk would be

$$\dot{m}(v_K - 2\pi\nu_s r) = r \frac{B_z B_\phi}{4\pi H} (4\pi H \delta r). \quad (1)$$

where v_K is the Keplerian orbit speed and ν_s the spin frequency of the central object. The conventional expression for the magnetosphere radius can be obtained with two additional assumptions: (i) that the field is fundamentally a dipole field

that is reshaped by the surface currents of the inner disk and (ii) that $B_\phi = \lambda B_z(1 - 2\pi\nu_s r/v_k)$, where λ is a dimensionless constant of order unity. This form accounts for the obvious facts that B_ϕ should go to zero at r_c , change sign there and grow in magnitude at greater distances from r_c . In fact, however, we should note that we are only describing an average B_ϕ here, because it is possible that the field lines become overly stretched by the mismatch between magnetospheric and Keplerian disk speeds, then break and reconnect across the disk. This type of behavior leads to high frequency oscillations and has been described in numerical simulations. With these assumptions we obtain

$$r = \left(\frac{\lambda\delta r}{r}\right)^{2/7} \left(\frac{\mu^4}{GM\dot{m}^2}\right)^{1/7} \quad (2)$$

In order to estimate $\delta r/r$, we choose an object for which few would quibble about it being magnetic; namely an atoll class NS. The rate of spin is typically 400 - 500 Hz, the co-rotation radius is ~ 26 km, and the maximum luminosity for the low state is $\sim 2 \times 10^{36} = GM\dot{m}/2r$ erg/s, from which $\dot{m} = 5.5 \times 10^{16}$ g/s, for $M = 1.4M_\odot$. For a magnetic moment of $\sim 10^{27}$ gauss cm³, we find that $(\frac{\lambda\delta r}{r})^{2/7} \sim 0.3$. Thus if $\lambda \sim 1$, then $\delta r/r \sim 0.013$; i.e., the boundary region is suitably small, though larger than the scale height of the trailing disk. In this small region the flow changes from co-rotation with the magnetosphere to Keplerian. When its inner radius is inside r_c , its weight is not entirely supported by centrifugal forces and it provides the ‘dead-weight’ against the magnetopause.

APPENDIX

D. New Observations

The equations used in our previous work (Robertson & Leiter 2002) are repeated here for analysis of a few new observations. Using units of 10^{27} gauss cm³ for magnetic moments, 100 Hz for spin, 10^6 cm for radii, 10^{15} g/s for accretion rates, solar mass units, $\lambda\delta r/r = 0.013$ and otherwise obvious notation, we found the magnetosphere radius to be (Equation (2), Appendix C):

$$r_m = 8 \times 10^6 \left(\frac{\mu_{27}^4}{m\dot{m}_{15}^2}\right)^{1/7} \text{ cm} \quad (1)$$

A co-rotation radius of:

$$r_c = 7 \times 10^6 \left(\frac{m}{\nu^2}\right)^{1/3} \text{ cm} \quad (2)$$

The low state luminosity at the co-rotation radius:

$$L_c = 1.5 \times 10^{34} \mu_{27}^2 \nu_2^3 m^{-1} \text{ erg/s} \quad (3)$$

High state luminosity for accretion reaching the central object:

$$L_s = \xi \dot{m} c^2 = 1.4 \times 10^{36} \xi \mu_{27}^2 \nu_2^{7/3} m^{-5/3} \text{ erg/s} \quad (4)$$

Where $\xi \sim 1$ for MECO and $\xi = 0.14$ for NS is the efficiency of accretion to the central surface. We calculate the quiescent luminosities in the soft x-ray band from 0.5 - 10 keV using the correlations of Possenti et al. (2001) with spin-down energy loss rate as:

$$L_q = \beta \dot{E} = \beta 4\pi^2 I \nu \dot{\nu} \quad (5)$$

where I is the moment of inertia of the star, ν its rate of spin and β a multiplier that can be determined from the new $\dot{E} - L_q$ correlation for given \dot{E} ; i.e., known spin and magnetic moment. (In previous work we had used $\beta = 10^{-3}$ for all objects.) We assume that the luminosity is that of a spinning magnetic dipole for which $\dot{E} = 32\pi^4 \mu^2 \nu^4 / 3c^3$, (Bhattacharya & Srinivasan 1995) where μ is the magnetic moment. Thus the quiescent x-ray luminosity would then be given by :

$$L_q = \beta \times \frac{32\pi^4 \mu^2 \nu^4}{3c^3} = 3.8 \times 10^{33} \beta \mu_{27}^2 \nu_2^4 \text{ erg/s} \quad (6)$$

As the magnetic moment, μ_{27} , enters each of the luminosity equations it can be eliminated from ratios of these luminosities, leaving relations involving only masses and spins. For known masses, the ratios then yield the spins. Alternatively, if the spin is known from burst oscillations, pulses or spectral fit determinations of r_c , one only needs one measured luminosity to enable calculation of the remaining μ_{27} and L_q . For most GBHC, we found it to be necessary to estimate the co-rotation radius from multicolor disk fits to the thermal component of low state spectra. The reason for this is that the luminosities are seldom available across the whole spectral hardening transition of GBHC. For GBHC, it is a common finding that the low state inner disk radius is much larger than that of the marginally stable orbit (e.g. Markoff, Falcke & Fender 2001, Życki, Done & Smith 1997a,b 1998, Done & Życki 1999, Wilson & Done 2001). The presence of a magnetosphere is an obvious explanation. Given an inner disk radius at the spectral state transition, the GBHC spin frequency follows from the Kepler relation $2\pi\nu_s = \sqrt{GM/r^3}$.

Data:

The third accreting millisecond pulsar, **XTE J0929-314** has been found (Galloway et al. 2002) with $\nu_s = 1/P = 185$

Hz and period derivative $\dot{P} = 2.69 \times 10^{-18}$, from which the magnetic field (calculated as $3.2 \times \sqrt{P\dot{P}}$) is 3.9×10^9 gauss. This is typical of a Z source. Assuming a NS radius of 13 km, the magnetic moment is $BR^3 = 8.5 \times 10^{27}$ gauss cm³. The calculated low state limit co-rotation luminosity is $L_c = 4.9 \times 10^{36}$ erg/s. Approximately 40% of this would be the luminosity in the (2 - 10 keV) band. This yields an expected flux of 2×10^{-10} erg/cm²/s for a distance of 9 kpc. This corresponds to the knee of the published light curve where the luminosity begins a rapid decline as the propeller becomes active. Similar breaking behavior has been seen in Sax J1808.4-3659 and GRO J1655-40 at propeller onset. The predicted 0.5-10 keV band luminosity is $L_q = 1.3 \times 10^{33}$ erg/s.

The second accreting millisecond pulsar **XTE J1751-305** was found with a spin of 435 Hz. (Markwardt et al. 2002) Its spectrum has been analyzed (Miller et al. 2003). We find a hard state luminosity of 3.5×10^{36} erg/s ($d = 8$ kpc) at the start of the rapid decline which is characteristic of the onset of the propeller effect. We take this as an estimate of L_c . From this we estimate a magnetic moment of 1.9×10^{27} gauss cm³ and a quiescent luminosity of 5×10^{33} erg/s. An upper limit on quiescent luminosity of 1.8×10^{34} erg/s can be set by the detections of the source in late April 2002, as reported by Markwardt et al. (2002).

The accreting x-ray pulsar, **GRO J1744-28** has long been cited for exhibiting a propeller effect. Cui (1997) has given its spin frequency as 2.14 Hz and a low state limit luminosity as $L_c = 1.8 \times 10^{37}$ erg/s (2 - 60 keV.), for a distance of 8 kpc. These imply a magnetic moment of 1.3×10^{31} gauss cm³ and a magnetic field of $B = 5.9 \times 10^{12}$ gauss for a 13 km radius. Its spin-down energy loss rate should be $\dot{E} = 1.4 \times 10^{35}$ erg/s and its quiescent luminosity, $L_q = 3 \times 10^{31}$ erg/s. Due to its slow spin, GRO J1744-28 has a large co-rotation radius of 280 km. A mass accretion rate of $\dot{m} = 5.4 \times 10^{18}$ g/s is needed to reach L_c . Larger accretion rates are needed to reach the star surface, but such rates distributed over the surface would produce luminosity in excess of the Eddington limit. The fact that the magnetic field is strong enough to funnel a super-Eddington flow to the poles is the likely reason for the type II bursting behavior sometimes seen for this source. In addition to its historical illustration of a propeller effect, this source exemplifies the inverse correlation of spin and magnetic field strength in accreting sources. It requires a weak field to let an accretion disk get close enough to spin up the central object. For this reason we expect Z sources with their stronger B fields to generally spin more slowly than atolls.

The accreting pulsar, **4U0115+63**, with a spin of 0.276 Hz and a magnetic field, derived from its period derivative, of 1.3×10^{12} gauss (yielding $\mu = 2.9 \times 10^{30}$ gauss cm³ for a 13 km radius) has been shown (Campana et al. 2002) to exhibit a magnetic propeller effect with a huge luminosity interval from $L_c = 1.8 \times 10^{33}$ erg/s to $L_{min} = 9.6 \times 10^{35}$ erg/s. L_c held steady precisely at the calculated level for a lengthy period before luminosity began increasing. Due to the slow spin of this star, its quiescent luminosity, if ever observed, will be just that emanating from the surface. Its spin-down luminosity will be much too low to be observed.

The atoll source **4U1705-44** has been the subject of a recent study (Barret & Olive 2002) in which a Z track has been displayed in a color-color diagram. Observations labeled as 01 and 06 mark the end points of a spectral state transition for which the luminosity ratio $L_{min}/L_c = 25.6 \times 10^{36}/6.9 \times 10^{36} = 3.7$ can be found from their Table 2. These yield $\nu = 470$ Hz and a magnetic moment of $\mu = 2.5 \times 10^{27}$ gauss cm³. The spin-down energy loss rate is 1.2×10^{37} erg/s and the 0.5 - 10 keV quiescent luminosity is estimated to be about 5×10^{33} erg/s. At the apex of the Z track (observation 12), the luminosity was 2.4×10^{37} erg/s (for a distance of 7.4 kpc.); i.e., essentially the same as L_{min} . Although 4U1705-44 has long been classified as an atoll source, it is not surprising that it displayed the Z track in this outburst as its 0.1 - 200 keV luminosity reached 50% of the Eddington limit.

Considerable attention was paid to reports of a truncated accretion disk for the GBHC, **XTE J1118+480** (McClintock et al 2001) because of the extreme interest in advective accretion flow (ADAF) models for GBHC (Narayan, Garcia & McClintock 1997). McClintock et al, fit the low state spectrum to a disk blackbody plus power law model and found that the disk inner radius would be about $35R_{schw}$, or 720 km for $7 M_\odot$. Using this as an estimate of the co-rotation radius we find the spin to be 8 Hz. The corresponding low state luminosity of 1.2×10^{36} erg/s (for $d = 1.8$ kpc) lets us find a magnetic moment of 10^{30} gauss cm³. The calculated spin-down energy loss rate is 1.5×10^{35} erg/s and the quiescent luminosity would be about 3×10^{31} erg/s.

A rare transition to the hard state for **LMC X-3** (Soria, Page & Wu 2002, Boyd et al. 2000) yields an estimate of the mean low state luminosity of $L_c = 7 \times 10^{36}$ erg/s and the high state luminosity in the same 2 - 10 keV band is approximately 6×10^{38} erg/s at the end of the transition to the soft state. Taking these as L_c and L_{min} permits the estimates of spin $\nu = 16$ Hz and magnetic moment $\mu = 8.6 \times 10^{29}$ gauss cm³, assuming $7 M_\odot$. From these we calculate a quiescent luminosity of 10^{33} erg/s.

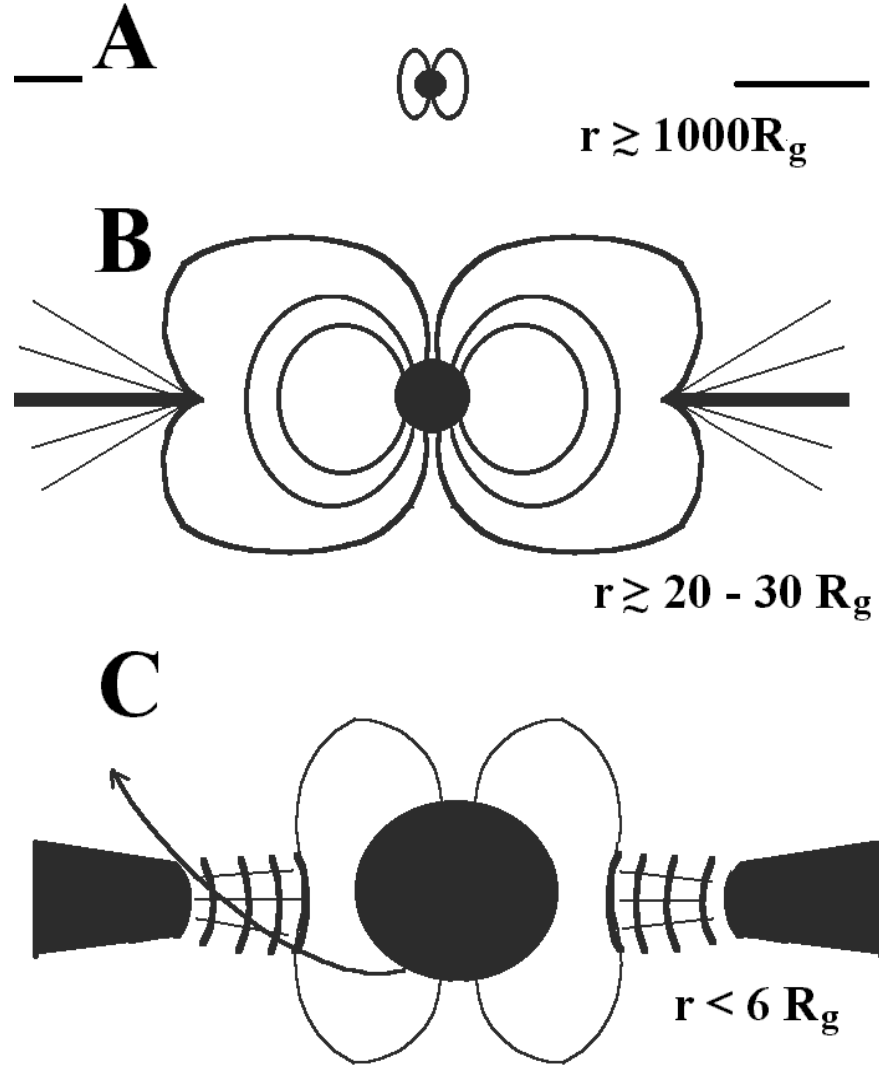


FIG. 1.— MECO Spectral States: **A quiescent:** Inner disk ablated, low accretion rate to inner ablation radius $\sim 10^9 - 10^{10} \text{ cm}$ generates optical emissions. Magnetic dipole radiation drives hard power-law x-ray spectrum. Cooling NS surface x-ray or quiescent MECO EUV emissions may be visible. **B. Low state:** Thin, gas pressure dominated inner disk has large magnetically dominated viscosity. The inner disk radius lies between the light cylinder and co-rotation radii. Disk winds and jets are driven by the magnetic propeller. A hard spectrum is produced as most soft x-ray photons from the disk are Comptonized by either outflow or corona. Outflows of electrons on open magnetic field lines produce synchrotron radiation. Most of the outer disk is shielded from the magnetic field of the central object as surface currents in the inner disk change the topology of the magnetopause. **C: High state:** Once the inner disk is inside the co-rotation radius, the outflow and synchrotron emissions subside. Relaxation oscillations may occur as radiation from the central object momentarily drives the inner disk back outside the co-rotation radius. A boundary layer of material beginning to co-rotate with the magnetosphere may push the magnetopause to the star surface for NS or inside r_{ms} for MECO, where a supersonic flow plunges inward until radiation pressure stabilizes the magnetopause or interchange instabilities break up the flow. The MECO photosphere radiates a bright ‘ultrasoft’ thermal component. Bulk Comptonization of many photons on spiral trajectories crossing the disk produces a hard x-ray spectral tail.